HHS Public Access

Author manuscript

*Ophthalmol Glaucoma*. Author manuscript; available in PMC 2023 May 01.

Published in final edited form as:

*Ophthalmol Glaucoma*. 2022 ; 5(3): 250–261. doi:10.1016/j.ogla.2021.10.005.

# Dynamic Alterations in Blood Flow in Glaucoma Measured with Laser Speckle Contrast Imaging

**Alfred Vinnett**[1,*], **Jayanth Kandukuri**[2,*], **Christopher Le**[1], **Kyoung-A Cho**[2], **Avigyan Sinha**[2], **Samuel Asanad**[1], **Ginger Thompson**[3], **Victoria Chen**[1], **Abhishek Rege**[2], **Osamah J Saeedi**[1,†]

[1]Department of Ophthalmology and Visual Sciences, University of Maryland Baltimore, Baltimore, Maryland, USA

[2]Vasoptic Medical, Inc., Baltimore, Maryland, USA

[3]Department of Ophthalmology/Hamilton Eye Institute, University of Tennessee Health Sciences Center, Memphis, Tennessee, USA

## Abstract

**Objective:** To assess the repeatability of blood flow velocity index (BFVi) metrics obtained with a recently FDA-cleared laser speckle contrast imaging device, the XyCAM RI, and characterize differences in these metrics between control, glaucoma suspect, and glaucoma subjects.

**Design:** Prospective observational study

**Participants:** 46 subjects (20 control, 16 glaucoma suspect, and 10 glaucoma; one eye per subject)

**Methods:** Key dynamic BFVi metrics–mean, peak, dip, volumetric rise index (VRI), volumetric fall index (VFI), time to rise (TtR), time to fall (TtF), blow out time (BOT), skew, acceleration time index (ATI)–were measured in the optic disc, optic disc vessels, optic disc perfusion region, and macula in four imaging sessions on the same day. Intrasession and intersession variability were calculated using the coefficient of variation (CV) for each metric in each region of interest (ROI). Values for each dynamic BFVi variable were compared between glaucoma subjects, glaucoma suspects, and controls using bivariate and multivariable analysis. Pearson correlation coefficients were used to correlate each variable in each ROI with age, intraocular pressure, cup to disc ratio, mean deviation, pattern standard deviation, retinal nerve fiber layer thickness, and minimum rim width.

[†]**Corresponding Author Information:** Osamah J. Saeedi, MD, 419 W. Redwood Street, Suite 470, Baltimore, MD 21201, Phone: 667-214-1232, osaeedi@som.umaryland.edu.

[*]Authors contributed equally

**Conflict of Interest:** JK, KC, AS, and AR were employed or contracted by Vasoptic Medical, Inc. when this work was performed. AR, JK, and KC have ownership interest in Vasoptic Medical, Inc. AR and JK are inventors on patents pertaining to the speckle-based blood flow monitoring technology.

**Main outcome measures:** CV for the intrasession and intersession variability for each dynamic BFVi metric in each ROI, and differences in each metric in each ROI between each diagnostic group.

**Results:** The intersession CV for mean, peak, dip, as well as VRI, VFI, TtR, and TtF ranged from 3.2 ± 2.5% to 11.0 ± 3.8%. Age, cup-to-disc ratio, optical coherence tomography metrics, and visual field metrics showed significant correlations with dynamic BFVi variables. Peak, mean, dip, VRI, and VFI, were significantly lower in glaucoma subjects than in control subjects in all ROI except the fovea. These metrics were also significantly lower in glaucoma subjects than suspects in the disc vessels.

**Conclusions:** Dynamic blood flow metrics measured with the XyCAM RI are reliable, associated with structural and functional glaucoma metrics, and significantly different between glaucoma subjects, glaucoma suspects, and controls. The XyCAM RI may serve as an important tool in glaucoma management in the future.

## Précis

A novel laser speckle contrast imaging device reproducibly measures dynamic ocular blood flow in the optic nerve head and macula. Dynamic blood flow metrics were lower in glaucoma subjects as compared to suspects and controls.

### Keywords

ocular blood flow; optic nerve head; macula; laser speckle contrast imaging; glaucoma

Despite advances in glaucoma therapy, many patients continue to irreversibly lose vision due to the disease, indicating the need for better biomarkers. Automated perimetry remains central to the management of patients with glaucoma, but has notable limitations including testing variability, long duration, and a substantial subset of patients who are unable to perform reliable visual field testing. Furthermore, the COVID-19 pandemic raised concerns of the spread of pathogens with use of the perimetry bowl and challenges associated with cleaning it.[1]

Reliable measurement of blood flow at the optic nerve head and retina may present an alternative or complementary functional glaucoma biomarker.[2] Strong evidence supports a vascular component to the development and progression of glaucoma.[3-5] Vascular structural parameters such as vessel density or vessel caliber are reduced in glaucoma.[6] Measurement of dynamic ocular blood flow metrics such as mean, maximal, and minimal blood flow in the optic nerve head and macula may be more precise than structural biomarkers and further hold the promise of being reversible.[7,8] However, widespread adoption of prior technologies that measure dynamic ocular blood flow has been limited due to low reproducibility, high cost, and instrument complexity.

The XyCAM RI (Vasoptic Medical, Inc., Baltimore, MD) is a high-speed, portable ocular blood flow imaging system with high repeatability that has recently been cleared by the Food and Drug Administration (FDA) in the United States.[9,10] This device uses Laser Speckle Contrast Imaging (LSCI) to measure dynamic changes in ocular blood flow. LSCI

is a noninvasive technique that uses a safe, low-intensity laser to illuminate the posterior segment leading to speckle formation in the acquired image data. Because of red blood cell motion within blood vessels, a blurring effect is observed in the speckle pattern, the extent of which can be quantified to obtain estimates of blood flow velocity information with high spatiotemporal resolution. The device has been used in a portable manner at two sites and demonstrated high measurement repeatability at each site despite frequent transport and installation between the two sites.[9] In this study, we use the XyCAM RI to assess macular and optic nerve head (ONH) blood flow in healthy, glaucoma suspect, and glaucoma subjects for two aims: first, to determine the repeatability of dynamic blood flow measurements in glaucoma, glaucoma suspects, and control subjects, and second, to determine the ability of the XyCAM RI to differentiate controls from glaucoma suspect and glaucoma subjects using temporal characteristics of dynamic blood flow patterns.

## Methods

### Study Design

We conducted a prospective observational study in the Department of Ophthalmology and Visual Sciences at the University of Maryland Baltimore (UMB). All clinical experimentation was performed in compliance with the tenets of the Declaration of Helsinki, and with approvals from the UMB Institutional Review Board.

### Participants

Individuals were screened and recruited from the faculty practice of the Department of Ophthalmology and Visual Sciences: control subjects from the optometry practice and glaucoma or glaucoma suspect subjects from the glaucoma practice. Informed consent was obtained from all participants. Institutional Review Board (IRB) approval was obtained for this study, and this study adhered to Declaration of Helsinki tenets. Subjects received monetary compensation for their participation. Inclusion criteria included age 21 or older with binocular vision. Glaucoma subjects were required to have at least one eye with moderate to severe glaucoma as defined by Hodapp-Anderson-Parrish criteria.[11] We excluded patients from the study if they had visually significant media opacity, anatomically narrow angles, prior adverse reaction to tropicamide or fluorescein, greater than 15 diopters of refractive error, were pregnant or nursing, had an implantable device, or had prior ocular surgery other than uncomplicated cataract or glaucoma surgery. We screened and approached 94 subjects to enroll for the study. Forty-seven subjects consented and enrolled in the study: 20 healthy controls, 16 glaucoma suspects, and 11 glaucoma subjects. One glaucoma subject was ultimately excluded from analysis for having previous retinal laser. One subject had both eyes imaged, and one eye was chosen for analysis at random. One glaucoma subject had previous successful glaucoma surgery and the other nine subjects had no prior glaucoma surgery. There was no significant difference in age, race, sex, or diagnosis between the screened patients who were not included in the study and the enrolled subjects in the study (Supplemental Table S1). One subject's macular data was excluded from analysis due to poor image quality. An experienced glaucoma specialist (OJS) reviewed clinical data of all subjects including visual fields and spectral domain ocular coherence tomography (SD-OCT) of the retinal nerve fiber layer (RNFL) and macula. Subjects were

classified as glaucoma or glaucoma suspect based on the preferred practice patterns of the American Academy of Ophthalmology.[12,13] Control subjects had a normal OCT RNFL, cup-to-disc ratio less than 0.5, and intraocular pressure (IOP) less than 21 mm Hg.

### Acquisition of XyCAM RI Imaging Data

The XyCAM RI is a portable ocular blood flow imager weighing 2.4 kg with a resolution of approximately 50 linear pixels per degree of field of view. For this study, the device was mounted on a slit-lamp base for stabilized use as in traditional ophthalmic photography settings. The XyCAM RI emits a near infrared (NIR, peak wavelength of 785 ± 10 nm) laser to enable LSCI of the subject's retina. Upon adjusting the field of view and focus, the operator triggered the acquisition of a sequential stack of speckle images for a duration of six seconds, with synchronous acquisition of a plethysmogram from a finger pulse oximeter for reference. Speckle images were acquired at a frame rate of 82 frames per second to capture the temporal dynamics with high resolution.

In each subject, the XyCAM RI was used to capture dynamic blood flow data from a field of view (FOV) of at least 20 degrees approximately centered on the ONH or macula or sequentially on both. To assess intersession repeatability of measurements, subjects underwent a total of four imaging sessions for each FOV, with a few minutes between the imaging sessions, but involving no significant activity from the subject that might influence ophthalmic blood flow. Data from both ONH and macular FOVs were acquired by a single operator in all glaucoma subjects and glaucoma suspect and in ten out of twenty control subjects. Among the remaining ten control subjects, three distinct operators imaged the ONH FOV only in five subjects and the macula FOV only in the other five subjects. The use of multiple operators permitted assessment of reproducibility across operators.

### Clinical Assessment

We performed standard clinical examination on each recruited subject including slit lamp examination, dilated fundus examination with assessment of cup-to-disc ratio, applanation tonometry, and gonioscopy. Vital signs including blood pressure, pulse, and continuous pulse oximetry were recorded. Glaucoma and glaucoma suspects underwent standard automated perimetry with a 24-2 Humphrey visual field (Zeiss Meditec, Dublin, California). All enrolled subjects underwent OCT RNFL, OCT Macula, and ONH analysis with minimum rim width (MRW) determination using SD-OCT with the Heidelberg Spectralis OCT2 (Heidelberg Engineering, Heidelberg, Germany). All visual fields were reliable with less than 15% false-positive errors and less than 20% fixation losses.[14] All SD-OCT scans had a quality rating of at least 20 (although generally above 25). This quality standard has been shown to have a high degree of accuracy in diagnosing early glaucoma.[15]

### Laser Speckle Contrast Imaging Analysis

The XyCAM RI outputs a time-stack of blood flow velocity index (BFVi) maps of the FOV by processing the raw data obtained under laser illumination and provides a time-sequence of BFVi values at each pixel. BFVi, expressed in arbitrary units, is depicted in pseudo-color to display the blood flow status in the FOV as shown in Figure 1. The speckle image dataset was registered prior to BFVi estimation to compensate for motion artifacts. We selected

specific regions of interest (ROIs) using XyCAM RI analysis tools. In data acquired from ONH imaging, we manually identified the optic disc and further segmented the disc into two additional ROIs: visually discriminable vessels within the optic disc (disc vessels) and the remaining background areas of the optic disc without discriminable vessels (disc perfusion) (Figure 2). In data acquired from macular imaging, we manually identified the fovea and analyzed a circular ROI with a diameter of 250 pixels (~5-degree FOV with diameter of ~1.5mm) centered on the fovea. We computed and plotted the mean BFVi value within each ROI and each frame on the time axis to reveal temporal 6-second sequences of BFVi values ("waveforms") as shown in Figure 3. These waveforms are pulsatile, revealing peaks and dips in BFVi values as blood flow to the retina increases and decreases synchronously with every heartbeat.[9,16] We manually identified cycles within the waveform, defined as a sequence of BFVi values from one dip to the next dip through a peak, and cycles that contained significant imaging artifacts (e.g., eye blinks, eye movement, or corneal reflection) were rejected and not considered for analysis.

## Waveform analysis

For each cycle, we noted BFVi values at various phases of the cycle and computed the average BFVi at the two dip locations of the cycle (dip BFVi), BFVi values averaged over an entire cycle (mean BFVi), and BFVi at the peak (peak BFVi) for each ROI and used these BFVi variables for further analysis. Derivative metrics were also computed such as volumetric rise index (VRI) and volumetric fall index (VFI) defined by the area under the BFVi waveform during its rising and falling phases, respectively. Time-to-rise (TtR) measures the time in milliseconds from Dip 1 to the peak, while time-to-fall (TtF) measures the time in milliseconds from the peak to Dip 2 in milliseconds. Figure 3 provides an illustration of all XyCAM RI computed waveform-based metrics that are provided to the user. Additionally, we computed offline certain pulse waveform parameters that are not automatically output by the XyCAM RI, but have been reported in previous studies using the LSFG-NAVI (Softcare Co., Ltd., Fukuoka, Japan), another speckle-based ocular imaging instrument.[8,17,18] Specifically, we computed blow-out time (BOT), acceleration time index (ATI), and skew using equations described in Figure 3.[19]

## Statistical Analysis:

We assessed repeatability of BFVi measurements by calculating the intrasession and intersession coefficient of variation (CV). We calculated the intrasession CV within an imaging session as the variation across multiple cycles within the same imaging session of six second duration. The intersession CV was calculated across the multiple imaging sessions. We compared all mean values of ocular blood flow metrics across healthy controls, glaucoma suspect, and glaucoma subject groups using ANOVA (analysis of variance), and if significant ($p<0.05$), compared pairwise differences in the three groups with the Tukey-Kramer test. We calculated Pearson correlation coefficients to reflect the association between BFVi measurements and traditional risk factors and indicators of glaucoma including age, intraocular pressure (IOP), cup-to-disc ratio, OCT metrics such as mean rim width (MRW) and overall RNFL thickness, and visual field metrics including MD24-2 (dB) and PSD24-2 (dB). We determined significance ($p<0.05$) using a two-tailed t-test. We then conducted a linear regression for each dynamic BFVi parameter in each region (optic disc,

disc vessels, disc perfusion, fovea) with diagnosis as the independent variable and the BFVi parameter as the dependent variable accounting for age and sex. We determined statistical significance ($p<0.05$) using a Wald test.

We then explored whether a combination of dynamic BFVi parameters found to be significant in our multivariable linear regression and the demographic variables of sex and age could improve the ability to differentiate glaucoma subjects, suspects, and control subjects than these features alone. We conducted a Factor Analysis of Mixed Data (FAMD) analysis, a dimensionality reduction technique which combines principal component analysis (PCA) and multiple correspondence analysis (MCA) and allows for inclusion of both continuous and categorical variables. This analysis decomposed BFVi and demographic variables into two orthogonal vectors using unsupervised methods and is necessary due to the collinearity BFVi variables. We then evaluated the fit of these FAMD components to differentiate disease status and compared their performance to logistic regression with each of the BFVi dynamic parameters individually. FAMD statistical analysis was performed with R 4.0.3 (R foundation for Statistical Computing).[20,21]

## Results

### Patient Demographics

We completed imaging and data analysis in a total of 46 subjects. Table 1 shows the demographic and clinical characteristics of our sample. Control subjects were significantly younger ($p < 0.05$). There were more males in the glaucoma group (70%) and more females in the glaucoma suspect group (75%), but the differences in distribution ($p = 0.08$) did not meet our criteria for statistical significance. We accounted for these differences in our multivariable analysis.

### Repeatability of BFVi measurements

Intrasession repeatability of BFVi measurements for the optic disc, disc vessels, disc perfusion, and fovea is represented by the CVs listed in Table 2 for each group of subjects. Dip, mean, peak, VRI, VFI, TtR, and TtF showed high repeatability for all fields of view and populations. Of these variables, the lowest intrasession CV was 1.8 ± 0.7% in the mean BFVi in the optic disc ROI for healthy controls, and the highest was 9.0 ± 4.2 for VRI in the macula. Of all metrics, skew had the highest variability in each ROI and condition with the highest CV of 20.4 ± 11.5% in the fovea region for glaucoma suspects. Tukey-Kramer tests revealed a significantly higher intrasession variability ($p < 0.05$) in glaucoma subjects than in control subjects with respect to dip, mean, VFI, and TtF measurements in the optic disc, disc vessel, and disc perfusion regions.

The intersession repeatability of BFVi measurements was similarly high in the dip, mean, peak, VRI, VFI, TtR, and TtF metrics with a highest CV of 11.0 ± 3.8% for VRI in the disc perfusion ROI for glaucoma subjects (Table 3). Of all metrics, skew had the highest variability in each ROI and condition with the highest CV of 14.6 ± 14.7% in the disc vessel ROI for glaucoma suspects. There were fewer significant differences in intersession CV for all BFVi measurements across the three subject groups, with only VRI measurements in

disc vessels and skew, ATI, and BOT measurements in the fovea having significantly higher intersession variability in glaucoma than control subjects.

## Correlations with Glaucoma Status

Observed BFVi measurements in each of the four ROIs of healthy control, glaucoma suspect, and glaucoma subjects are shown in Table 4. Dip, mean, peak, VRI, and VFI measurements were significantly different between groups in the entire optic disc (greatest in controls, followed by suspects, and then glaucoma subjects). All of these measurements except VRI were significantly different in the disc vessel ROI. In the disc perfusion ROI, which excludes major vessels, dip, mean, and VFI were significantly different between groups. Metrics obtained from the foveal ROI were significantly different only in skew and BOT. Significance of pairwise comparisons of the three subject groups using Tukey-Kramer tests confirm that a number of metrics reveal statistical differences between the healthy control and glaucoma groups, while dip and mean in disc vessels provide additional discrimination of glaucoma suspect subjects from glaucoma subjects (Supplemental Figure S1). In all cases for dip, mean, peak, VRI, VFI metrics, means were lower in glaucoma subjects than in healthy control subjects and those for glaucoma suspect subjects lay between the glaucoma and healthy control groups.

Supplemental Tables 2A-C show Pearson correlation coefficients stratified by group between BFVi measurements and certain established risk factors and features of glaucoma including age, intraocular pressure (IOP), cup-to-disc ratio, MRW, overall RNFL thickness, MD, and PSD. In all groups, there was no correlation between BFVi measurements and IOP in any ROI. Skew and BOT were generally correlated with age in multiple ROIs in all groups. Among control subjects, dip, mean, and peak were correlated with cup-to-disc ratio in the optic disc and disc vessel ROI, while in the disc perfusion ROI, peak and VRI were correlated with RNFL and dip alone was correlated with cup-to-disc ratio. Among glaucoma suspect subjects, BOT was correlated with MD in all ROI excluding fovea. Peak was correlated with RNFL only in the disc vessels ROI. Finally, among glaucoma subjects, we observed significant correlations between skew and BOT with MD in all ROI. We also observed significant correlations between OCT parameters and dip, mean, and peak in all ROI excluding the fovea. These same BFVi variables were also correlated with PSD in the optic disc and disc vessels ROI.

Table 5 shows results of the multivariable linear regression accounting for age and sex in all ROIs. We confirmed that the standard assumptions for linear regression such as normality and homoscedasticity held in all regressions. We corrected for non-normality by log transforming three variables within the disc perfusion ROI (dip, VRI, and VFI). None of the BFVi variables were significantly different in the fovea ROI. In the optic disc ROI, peak, dip, mean, VRI, and VFI were significantly lower in glaucoma subjects as compared to controls in all three optic nerve head ROIs (optic disc, disc vessels, disc perfusion). In the disc vessel ROI, peak, dip, mean, VRI, and VFI were significantly different for all three subgroups, specifically highest in controls, lower in glaucoma suspects, and lowest in glaucoma subjects. When we repeated the analysis excluding a glaucoma subject who had a prior tube shunt, significant BFVi variables did not change.

### Factor Analysis of Mixed Data (FAMD) Analysis:

We used FAMD, an unsupervised machine learning method that mixes principal component analysis (PCA) and multiple correspondence analysis (MCA) to balance consideration of continuous and categorical variables, to decompose BFVi parameters that were significant in the multivariable analysis for the disc vessel region (peak, dip, mean, VRI, and VFI) and demographic variables into orthogonal vectors, Dim1 and Dim2. Together, Dim1 and Dim2 accounted for 79.8% of the variance within the data. Dim1 was primarily comprised of dynamic BFVi parameters and Dim2 included only age and sex (Supplemental Figure S2). Using binomial logistic regression to compare controls and glaucoma subjects, we found that higher BFVi parameters (Dim1) increased the chance of being a control subject ($p = 0.02$) with no significant effect of age and sex (Dim2, $p = 0.14$). Using the same method to compare glaucoma subject and glaucoma suspects, we found that higher BFVi parameters were associated with a higher likelihood of being a glaucoma suspect ($p = 0.03$), and that higher Dim2 (consisting of age and sex) increased chances of being a control subject ($p = 0.04$).

In order to assess whether combining BFVi parameters would enable a logistic regression model to better discriminate between control and glaucoma status, we compared Nagelkerke's $R^2$ for the bivariate binomial logistic regression models between control and glaucoma subject status and each BFVi parameter, as well as Dim1 Dim1 had the higher $R^2$ (0.46) than any of the individual dip (0.40), mean (0.39), peak (0.32), VFI (0.30), VRI (0.25) BFVi parameters. Using the same method to compare glaucoma subject and glaucoma suspects, we found that Dim1 had a comparable $R^2$ (0.29) with the mean (0.29) and dip (0.30) variables and a greater $R^2$ than peak (0.22), VFI (0.12), and VRI (0.16) BFVi variables. This analysis reveals that BFVi parameters, when combined, may improve the determination of glaucoma diagnosis relative to the parameters alone.

## Discussion

Our study represents the first assessment of a new LSCI-based ocular imaging device, the XyCAM RI, in glaucoma subjects. We found that BFVi variables, when focused on the optic nerve head, were significantly different between controls, glaucoma suspects and glaucoma subjects. While LSCI has previously been used for ocular imaging for glaucoma, the XyCAM RI is a new platform with certain distinct features that may afford it an advantage over other devices.[8,22-24] The device is portable, has high temporal resolution of 82 frames per second, has high repeatability, and permits reliable, detailed assessment of ocular blood flow dynamics.[9] The high temporal resolution may also limit the effect of motion artifact on the entire measurement, unlike in OCT angiography, where data is aggregated over larger timescales to produce a single estimate of perfusion status at a specific location. We have previously observed that while LSCI-based mean BFVi and peak BFVi estimates demonstrates acceptable correlation with peripapillary perfusion density obtained using OCT-A, correlation is poor for dip BFVi estimates.[25]

The XyCAM RI and LSFG-NAVI are similar devices, but have some notable differences.[26] The XyCAM RI obtains blood flow information from a circular field of view of 25 degrees, while the field of view imaged by LSFG-NAVI is 21 degrees (horizontal) by 12 degrees

(vertical). The XyCAM RI has a spatial resolution of 48 pixels/degree, while the LSFG-NAVI has a spatial resolution of 35 pixels/degree. XyCAM RI has a temporal resolution of 82 Hz, compared to the LSFG-NAVI's temporal resolution of 30 Hz. The LSFG-NAVI uses a higher wavelength of 830nm which may results in a greater contribution from blood flow in the choroidal layers rather than in the retinal layers. Furthermore, the method of determining mean blur rate (MBR) is different – LSFG-NAVI uses exclusively spatial determination of MBR, whereas the XyCAM computes speckle contrast in the spatiotemporal domain.

### BFVi Measurements and Repeatability

Repeatability of the XyCAM RI in glaucoma, suspects, and controls is generally as good or better than previously reported methods of estimating ocular blood flow *in vivo*. For example, laser doppler imaging showed a CV of up to 37%, and the retinal function imager has a reported CV of 10.8% to 30.5%.[9,27-31] Reproducibility of LSCI imaging in this study is comparable with the repeatability of perfused vessel density measurements enabled by OCT angiography.[32] In our data, we found that while dip, mean, peak, VRI, VFI, TtR, and TtF were highly reproducible, other parameters such as skew had higher variability in comparison. This is consistent with previous reports of repeatability in waveform parameter measurements, where CV ranged from 1.86% to 11.19% and skew had higher CV than most other parameters.[8,19] The higher intrasession variability for BFVi metrics in glaucoma subjects is consistent with prior investigations showing higher variability in blood flow in glaucoma and provides further support for potential vascular dysregulation in glaucoma.[29,33-37]

### Role of blood flow dynamics in glaucoma assessment

Structural vascular measurements such as vessel density and vessel caliber have shown encouraging results as potential glaucoma biomarkers,[6] but our work shows that dynamic variables and flowrates may offer additional or complementary information. This makes a strong case to assess the role of temporally-resolved ocular blood flow dynamics for glaucoma assessment in larger clinical trials. Furthermore, prior work suggests the potential of decoupling between vessel density obtained by OCT-A and BFVi values obtained by XyCAM RI.[25] We further note that BFVi metrics used here, specifically dip, mean, peak, VFI, and VRI, performed better in terms of determining glaucoma status than those previously developed, specifically BOT and ATI, which have shown variable diagnostic efficacy between studies.[8,38,39] This may be because BOT and ATI are considered to be more closely correlated with systemic vascular resistance and cardiac parameters than with ocular status.[17,40-42] Supplemental Tables 2A-C reveal a much closer association between clinical glaucoma metrics in the optic disc ROIs as compared to the fovea ROI, consistent with our understanding of glaucoma as a primarily an axonopathy, but may also be due to contribution of choroidal flow to the imaging signal in the foveal region.

The present study is one of the few studies conducted in the United States and the only one in a multi-ethnic population with a large proportion of African Americans.[34] Prior studies have primarily been conducted in Asian and European populations.[8,17,19,38-40] Furthermore, the prior study conducted by Gardiner et al. in the United States did not report racial and ethnic data, but may have had proportionally fewer nonwhite subjects.[38] In their study,

Gardiner et al. showed increased blood flow in glaucoma suspects compared to controls or glaucoma subjects.[38] The difference in patient demographics may be one reason that our results differed, showing highest BFVi metrics in controls followed by glaucoma suspects, followed by glaucoma subjects with the lowest BFVi metrics. We also note that blood flow parameters may be affected by the degree of pigmentation within the retinal pigment epithelium, which was not adjusted for in our analysis. Previous studies with Color Doppler imaging and confocal scanning laser Doppler demonstrated lower blood flow in people of African descent compared to European descent and greater correlation between blood flow and ONH changes in glaucoma, potentially relating to the increased rate of glaucoma among African Africans.[43-48]

The breadth of metrics available with assessment of ocular blood flow dynamics with the XyCAM RI presents avenues to potentially better diagnose glaucoma early in the disease state and identify those most likely to develop the disease. While these metrics are highly colinear, we have shown that dip, mean, peak, VRI, and VFI in the optic vessels allow for differentiation of all 3 diagnostic groups from each other when accounting for the effects of age and sex. Furthermore, the FAMD analysis suggests that BFVi metrics in combination may offer improved discrimination between glaucoma subjects, suspects, and controls. However, the sample size in our study was limited, and an equivalent analysis in a larger clinical trial would be needed for more definitive results. A follow-up of glaucoma suspects is also needed to determine if BFVi metrics are able to assist in early assessment of risk of developing glaucoma.

Overall, our findings suggest the usefulness of assessing ocular blood flow dynamics for gathering insights on glaucoma status that may inform future strategies for glaucoma diagnostics and management. The XyCAM RI may fill an important clinical role in glaucoma diagnosis and management given that it is portable and noncontact. We plan to further assess whether the LSCI-based XyCAM RI can provide diagnostic classification with a high degree of confidence.

## Supplementary Material

Refer to Web version on PubMed Central for supplementary material.

## Financial Support:

OJS is supported by an NIH Career Development Award (K23EY025014) and R01EY031731. This study was supported in part from a grant from the Maryland Industrial Partnerships (MIPS) program, a portion of which was programmatically charged to Vasoptic Medical, Inc (VMI). VMI participated in the design of the study, conducting the study, data analysis, and reviewed the manuscript.

## Acronyms and Abbreviations:

| | |
|---|---|
| **ANOVA** | analysis of variance |
| **ATI** | acceleration time index |
| **BFVi** | blood flow velocity index |

| | |
|---|---|
| **BOT** | blow-out time |
| **CDR** | cup-to-disc ratio |
| **COVID** | coronavirus disease 2019 |
| **CV** | coefficient of variation |
| **FAMD** | Factor Analysis of Mixed Data |
| **FDA** | Food and Drug Administration |
| **FOV** | field of view |
| **FWHM** | full width half maximum |
| **IOP** | intraocular pressure |
| **LSCI** | laser speckle contrast imaging |
| **MBR** | mean blur rate |
| **MD** | mean deviation |
| **MRW** | minimum rim width |
| **NIR** | near infrared |
| **OCT** | optical coherence tomography |
| **ONH** | optic nerve head |
| **PCA** | principal component analysis |
| **PSD** | pattern standard deviation |
| **RNFL** | retinal nerve fiber layer |
| **ROI** | region of interest |
| **SD-OCT** | spectral domain ocular coherence tomography |
| **VFI** | volumetric fall index |
| **VRI** | volumetric rise index |

## References

1. Liebmann JM. Ophthalmology and glaucoma practice in the COVID-19 era. J Glaucoma. 2020;29(6):407–408. 10.1097/IJG.0000000000001519 [PubMed: 32301765]
2. Wang L, Cull GA, Piper C, Burgoyne CF, Fortune B. Anterior and posterior optic nerve head blood flow in nonhuman primate experimental glaucoma model measured by laser speckle imaging technique and microsphere method. Invest Ophthalmol Vis Sci. 2012;53(13):8303. 10.1167/iovs.12-10911 [PubMed: 23169886]

3. Abegão Pinto L, Willekens K, Van Keer K, Shibesh A, Molenberghs G, Vandewalle E, Stalmans I. Ocular blood flow in glaucoma - the Leuven Eye Study. Acta Ophthalmol (Copenh). 2016;94(6):592–598. 10.1111/aos.12962
4. Burgansky–Eliash Z, Bartov E, Barak A, Grinvald A, Gaton D. Blood-flow velocity in glaucoma patients measured with the retinal function imager. Curr Eye Res. 2016;41(7):965–970. 10.3109/02713683.2015.1080278 [PubMed: 26513272]
5. Promelle V, Daouk J, Bouzerar R, Jany B, Milazzo S, Balédent O. Ocular blood flow and cerebrospinal fluid pressure in glaucoma. Acta Radiol Open. 2016;5(2):205846011562427. 10.1177/2058460115624275
6. Yarmohammadi A, Zangwill LM, Diniz-Filho A, Suh MH, Manalastas PI, Fatehee N, Yousefi S, Belghith A, Saunders LJ, Medeiros FA, Huang D, Weinreb RN. Optical coherence tomography angiography vessel density in healthy, glaucoma suspect, and glaucoma eyes. Invest Ophthalmol Vis Sci. 2016;57(9):OCT451. 10.1167/iovs.15-18944 [PubMed: 27409505]
7. Fan N, Wang P, Tang L, Liu X. Ocular blood flow and normal tension glaucoma. BioMed Res Int. 2015;2015:308505. 10.1155/2015/308505 [PubMed: 26558263]
8. Shiga Y, Omodaka K, Kunikata H, Ryu M, Yokoyama Y, Tsuda S, Asano T, Maekawa S, Maruyama K, Nakazawa T. Waveform analysis of ocular blood flow and the early detection of normal tension glaucoma. Invest Ophthalmol Vis Sci. 2013;54(12):7699–7706. 10.1167/iovs.13-12930 [PubMed: 24130177]
9. Cho K-A, Rege A, Jing Y, Chaurasia A, Guruprasad A, Arthur E, Cabrera DeBuc D. Portable, non-invasive video imaging of retinal blood flow dynamics. Sci Rep. 2020; 10(1):20236. 10.1038/s41598-020-76407-5 [PubMed: 33214571]
10. Kalarn S, Cho K-A, Vinnett A, Asanad S, Baroni M, Pottenburgh J, Rege A, Saeedi O. Repeatability and reproducibility of the XyCAM RI across multiple operators. Invest Ophthalmol Vis Sci. 2020;61(7):5321–5321.
11. Hodapp E, Parrish RK, Anderson DR. Clinical Decisions in Glaucoma. Mosby Incorporated; 1993.
12. Prum BE, Rosenberg LF, Gedde SJ, Mansberger SL, Stein JD, Moroi SE, Herndon LW, Lim MC, Williams RD. Primary open-angle glaucoma Preferred Practice Pattern(®) guidelines. Ophthalmology. 2016;123(1):41–111. 10.1016/j.ophtha.2015.10.053
13. Prum BE, Lim MC, Mansberger SL, Stein JD, Moroi SE, Gedde SJ, Herndon LW, Rosenberg LF, Williams RD. Primary open-angle glaucoma suspect Preferred Practice Pattern® guidelines. Ophthalmology. 2016;123(1):112–151. 10.1016/j.ophtha.2015.10.055
14. Heijl A, Patella VM. Essential Perimetry: The Field Analyzer Primer. Carl Zeiss Meditec; 2002. Accessed June 27, 2021. http://lup.lub.lu.se/record/1124421
15. Pazos M, Dyrda AA, Biarnés M, Gómez A, Martín C, Mora C, Fatti G, Antón A. Diagnostic accuracy of spectralis SD OCT automated macular layers segmentation to discriminate normal from early glaucomatous eyes. Ophthalmology. 2017;124(8):1218–1228. 10.1016/j.ophtha.2017.03.044 [PubMed: 28461015]
16. Rege A, Liu Y, Jing Y, Howarth J, Brooke MJ, Saeedi O. Non-invasive imaging of retinal blood flow with high spatio-temporal resolution. Invest Ophthalmol Vis Sci. 2017;58(8):4851–4851.
17. Tsuda S, Kunikata H, Shimura M, Aizawa N, Omodaka K, Shiga Y, Yasuda M, Yokoyama Y, Nakazawa T. Pulse-waveform analysis of normal population using laser speckle flowgraphy. Curr Eye Res. 2014;39(12):1207–1215. 10.3109/02713683.2014.905608 [PubMed: 24749668]
18. Sugiyama T. Basic technology and clinical applications of the updated model of laser speckle flowgraphy to ocular diseases. Photonics. 2014;1(3):220–234. 10.3390/photonics1030220
19. Luft N, Wozniak PA, Aschinger GC, Fondi K, Bata AM, Werkmeister RM, Schmidl D, Witkowska KJ, Bolz M, Garhöfer G, Schmetterer L. Ocular blood flow measurements in healthy white subjects using laser speckle flowgraphy. PloS One. 2016;11(12):e0168190. 10.1371/journal.pone.0168190 [PubMed: 27959905]
20. R Core Team. R: A Language and Environment for Statistical Computing; 2020. https://www.R-project.org/
21. Lê S, Josse J, Husson F. FactoMineR: An R package for multivariate analysis. J Stat Softw. 2008;25(1):1–18. 10.18637/jss.v025.i01

22. Nagahara M, Tamaki Y, Tomidokoro A, Araie M. In vivo measurement of blood velocity in human major retinal vessels using the laser speckle method. Invest Ophthalmol Vis Sci. 2011;52(1):87. 10.1167/iovs.09-4422 [PubMed: 20702824]

23. Sugiyama T, Araie M, Riva CE, Schmetterer L, Orgul S. Use of laser speckle flowgraphy in ocular blood flow research. Acta Ophthalmol (Copenh). 2010;88(7):723–729. 10.1111/j.1755-3768.2009.01586.x

24. Wei X, Balne PK, Meissner KE, Barathi VA, Schmetterer L, Agrawal R. Assessment of flow dynamics in retinal and choroidal microcirculation. Surv Ophthalmol. 2018;63(5):646–664. 10.1016/j.survophthal.2018.03.003 [PubMed: 29577954]

25. Vinnett A, Asanad S, Cho K-A, Manalastas P, Rege A, Saeedi O. OCT Angiography vs laser speckle contrast imaging: correlation between static and dynamic measurements of peripapillary blood flow in glaucoma, glaucoma suspect, and healthy eyes. Invest Ophthalmol Vis Sci. 2020;61(7):617–617.

26. DeBuc DC, Rege A, Smiddy WE. Use of XyCAM RI for noninvasive visualization and analysis of retinal blood flow dynamics during clinical investigations. Expert Rev Med Devices. 2021;18(3):225–237. doi:10.1080/17434440.2021.1892486 [PubMed: 33635742]

27. Guan K, Hudson C, Flanagan JG. Variability and repeatability of retinal blood flow measurements using the Canon laser blood flowmeter. Microvasc Res. 2003;65(3):145–151. 10.1016/S0026-2862(03)00007-4 [PubMed: 12711255]

28. Chhablani J, Bartsch D-U, Cheng L, Gomez L, Alshareef RA, Rezeq SS, Garg SJ, Burgansky-Eliash Z, Freeman WR. Segmental reproducibility of retinal blood flow velocity measurements using retinal function imager. Graefes Arch Clin Exp Ophthalmol. 2013;251(12):2665–2670. 10.1007/s00417-013-2360-1 [PubMed: 23700326]

29. Aizawa N, Yokoyama Y, Chiba N, Omodaka K, Yasuda M, Otomo T, Nakamura M, Fuse N, Nakazawa T. Reproducibility of retinal circulation measurements obtained using laser speckle flowgraphy-NAVI in patients with glaucoma. Clin Ophthalmol. 2011;5:1171–1176. 10.2147/OPTH.S22093 [PubMed: 21887100]

30. Deng Y, Li M, Wang G, Jiang H, Wang J, Zhong J, Li S, Yuan J. The inter-visit variability of retinal blood flow velocity measurements using retinal function imager (RFI). Eye Vis (Lond). 2018;5:31. 10.1186/s40662-018-0124-z [PubMed: 30534577]

31. Cho K-A, Arthur E, Jing Y, Guruprasad A, Haghshenas SH, Rege A, DeBuc DC. Comparison of retinal blood velocity measurements using non-invasive retinal imagers. Invest Ophthalmol Vis Sci. 2019;60(9):5734–5734.

32. Lee M-W, Kim K-M, Lim H-B, Jo Y-J, Kim J-Y. Repeatability of vessel density measurements using optical coherence tomography angiography in retinal diseases. Br J Ophthalmol. 2019;103(5):704–710. 10.1136/bjophthalmol-2018-312516

33. Sugiyama T, Nakamura H. Increased short-term fluctuation in optic nerve head blood flow in a case of normal-tension glaucoma by the use of laser speckle flowgraphy. Vis (Basel). 2016;1(1):5. 10.3390/vision1010005

34. Prada D, Harris A, Guidoboni G, Siesky B, Huang AM, Arciero J. Autoregulation and neurovascular coupling in the optic nerve head. Surv Ophthalmol. 2016;61(2):164–186. 10.1016/j.survophthal.2015.10.004 [PubMed: 26498862]

35. Feke GT, Pasquale LR. Retinal blood flow response to posture change in glaucoma patients compared with healthy subjects. Ophthalmology. 2008;115(2):246–252. 10.1016/j.ophtha.2007.04.055 [PubMed: 17689612]

36. Galambos P, Vafiadis J, Vilchez SE, Wagenfeld L, Matthiessen ET, Richard G, Klemm M, Zeitz O. Compromised autoregulatory control of ocular hemodynamics in glaucoma patients after postural change. Ophthalmology. 2006;113(10):1832–1836. 10.1016/j.ophtha.2006.05.030 [PubMed: 16920194]

37. Pemp B, Georgopoulos M, Vass C, Fuchsjäger-Mayrl G, Luksch A, Rainer G, Schmetterer L. Diurnal fluctuation of ocular blood flow parameters in patients with primary open-angle glaucoma and healthy subjects. Br J Ophthalmol. 2009;93(4):486–491. 10.1136/bjo.2008.148676 [PubMed: 19029154]

38. Gardiner SK, Cull G, Fortune B, Wang L. Increased optic nerve head capillary blood flow in early primary open-angle glaucoma. Invest Ophthalmol Vis Sci. 2019;60(8):3110–3118. 10.1167/iovs.19-27389 [PubMed: 31323681]
39. Mursch-Edlmayr AS, Luft N, Podkowinski D, Ring M, Schmetterer L, Bolz M. Laser speckle flowgraphy derived characteristics of optic nerve head perfusion in normal tension glaucoma and healthy individuals: a pilot study. Sci Rep. 2018;8(1):5343. 10.1038/S41598-018-23149-0 [PubMed: 29593269]
40. Enomoto N, Anraku A, Tomita G, Iwase A, Sato T, Shoji N, Shiba T, Nakazawa T, Sugiyama K, Nitta K, Araie M. Characterization of laser speckle flowgraphy pulse waveform parameters for the evaluation of the optic nerve head and retinal circulation. Sci Rep. 2021;11(1):6847. 10.1038/s41598-021-86280-5 [PubMed: 33767305]
41. Shiba T, Takahashi M, Matsumoto T, Shirai K, Hori Y. Arterial stiffness shown by the cardio-ankle vascular index is an important contributor to optic nerve head microcirculation. Graefes Arch Clin Exp Ophthalmol. 2017;255(1):99–105. 10.1007/S00417-016-3521-9 [PubMed: 27743161]
42. Kobayashi T, Shiba T, Nishiwaki Y, Kinoshita A, Matsumoto T, Hori Y. Influence of age and gender on the pulse waveform in optic nerve head circulation in healthy men and women. Sci Rep. 2019;9(1): 17895. 10.1038/s41598-019-54470-x [PubMed: 31784662]
43. Congdon N, O'Colmain B, Klaver CCW, Klein R, Muñoz B, Friedman DS, Kempen J, Taylor HR, Mitchell P; Eye Diseases Prevalence Research Group. Causes and prevalence of visual impairment among adults in the United States. Arch Ophthalmol. 2004;122(4):477–485. 10.1001/archopht.122.4.477 [PubMed: 15078664]
44. Friedman DS, Wolfs RC, O'Colmain BJ, Klein BE, Taylor HR, West S, Leske MC, Mitchell P, Congdon N, Kempen J; Eye Diseases Prevalence Research Group. Prevalence of open-angle glaucoma among adults in the United States. Arch Ophthalmol. 2004;122(4):532–538. 10.1001/archopht.122.4.532 [PubMed: 15078671]
45. Kaskan B, Ramezani K, Harris A, Siesky B, Olinde C, WuDunn D, Eikenberry J, Tobe LA, Racette L. Differences in ocular blood flow between people of African and European descent with healthy eyes. J Glaucoma. 2016;25(9):709–715. 10.1097/IJG.0000000000000509 [PubMed: 27561101]
46. Siesky B, Harris A, Racette L, Abassi R, Chandrasekhar K, Tobe LA, Behzadi J, Eckert G, Amireskandari A, Muchnik M. Differences in ocular blood flow in glaucoma between patients of African and European descent. J Glaucoma. 2015;24(2):117–121. 10.1097/IJG.0b013e31829d9bb0 [PubMed: 23807346]
47. Kanakamedala P, Harris A, Siesky B, Tyring A, Muchnik M, Eckert G, Abrams Tobe L. Optic nerve head morphology in glaucoma patients of African descent is strongly correlated to retinal blood flow. Br J Ophthalmol. 2014;98(11):1551–1554. 10.1136/bjophthalmol-2013-304393 [PubMed: 24964797]
48. Siesky B, Harris A, Carr J, Verticchio Vercellin A, Hussain RM, Parekh Hembree P, Wentz S, Isaacs M, Eckert G, Moore NA. Reductions in retrobulbar and retinal capillary blood flow strongly correlate with changes in optic nerve head and retinal morphology over 4 years in open-angle glaucoma patients of African descent compared with patients of European descent. J Glaucoma. 2016;25(9):750–757. 10.1097/IJG.0000000000000520 [PubMed: 27561102]

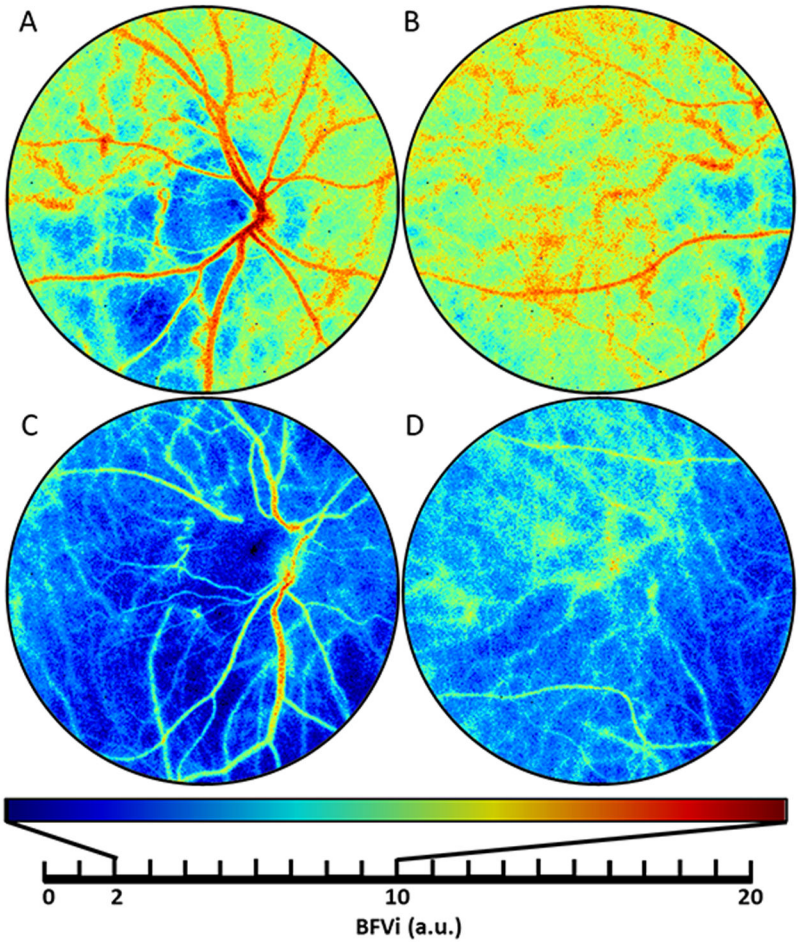


**Figure 1: Images of ocular blood flow obtained using the XyCAM RI.**

Blood flow velocity (BFV) images centered around the optic nerve head (ONH) and macula for a control subject (A, B) and a glaucoma subject (C, D). The same colormap scale is used across the subjects to display low flow velocities in cooler colors and high flow velocities in hotter colors.

a.u.: arbitrary units

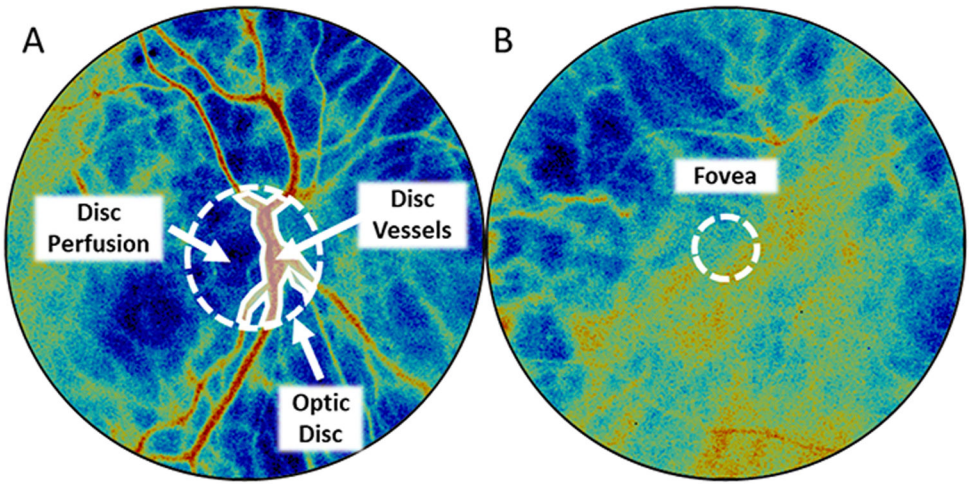


**Figure 2: Selection of assessed regions of interest.**

(A) To analyze flow-based metrics from the region of the optic nerve heard, three regions were selected: entire optic disc within the circular ROI, major blood vessels overlying the optic disc (disc vessels) delineated by the piecewise linear polygonal region, and the region of the optic disc not included within disc vessels (disc perfusion). (B) To analyze flow-based metrics from the foveal region, a fixed diameter region overlaying the fovea was selected.

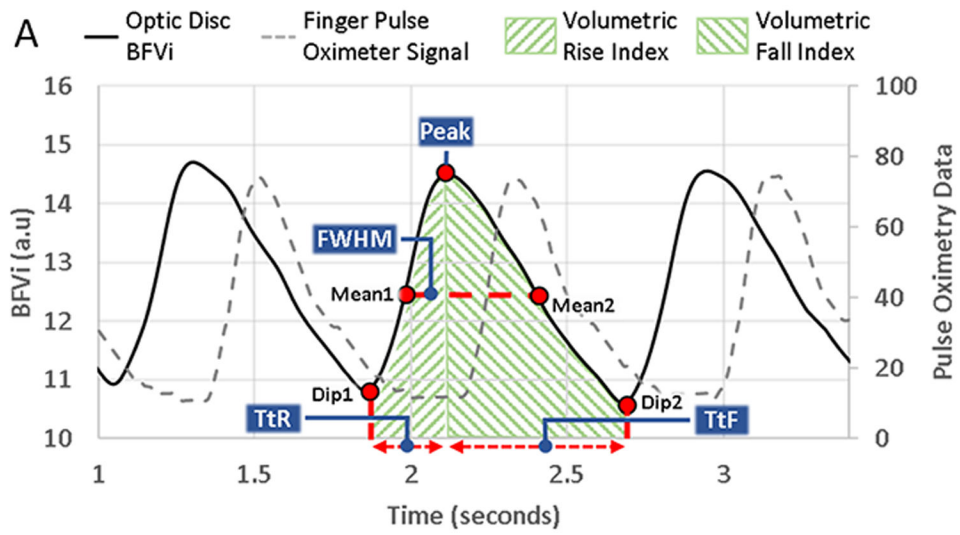


| B | |
|---|---|
| Mean = | 0.5 × (Mean1 + Mean2) |
| Dip = | 0.5 × (Dip1 + Dip2) |
| ATI = | TtR / (TtR + TtF) |
| BOT = | FWHM / (TtR + TtF) |
| FWHM = | Full-Width at 0.5 × (Peak-Dip) |
| Skewness = | $E \times [(k - \mu(k)) / \sigma(k)]^3$; where k is wave cycle, E is expected value, μ is the mean, σ is the standard deviation. |

**Figure 3: Illustration of a pulsatile blood flow velocity index (BFVi) waveform and computation of ocular blood flow metrics.**

Dip BFVi and peak BFVi pertain to phases corresponding to the cardiac diastole and systole. Mean BFVi corresponds to the average of the means of the rising and falling phase.

TtR: time-to-rise, TtF: time-to-fall, VRI: volumetric rise index (area under the rising portion of the BFVi waveform), VFI: volumetric fall index (area under the falling portion of the BFVi waveform), FWHM: full width half maximum, ATI: acceleration time index, BOT: blow-out time

**Table 1:**

**Subject demographics.**

Demographic distribution of imaged subjects and their clinical ophthalmic measurements relevant to diagnosis and management of glaucoma. (* indicates p-value < 0.05, ANOVA)
MD: mean deviation, PSD: pattern standard deviation, dB: decibel, OCT: optical coherence tomography, RNFL: retinal nerve fiber layer, MRW: mean rim width

| | Healthy Controls | Glaucoma Suspect | Glaucoma |
|---|---|---|---|
| **Age *** | 47.3 ± 16.5 | 59.6 ± 10.8 | 67.9 ± 6.8 |
| **Race** | | | |
| Black | 7(35%) | 8(50%) | 6(60%) |
| Non-Black | 13(65%) | 8(50%) | 4(40%) |
| **Sex** | | | |
| Male | 9(45%) | 4(25%) | 7(70%) |
| Female | 11(55%) | 12(75%) | 3(30%) |
| **Intraocular Pressure** | 14.5 ± 3.6 | 16.1 ± 3.9 | 16.4 ± 4.7 |
| **Cup-to-Disc Ratio *** | 0.31 ± 0.10 | 0.59 ± 0.16 | 0.71 ± 0.22 |
| **Visual Field Metrics** | | | |
| MD 24-2 (dB)* | N/A | −0.34 ± 1.96 | −10.03 ± 6.22 |
| PSD 24-2 (dB)* | N/A | 1.86 ± 0.76 | 8.82 ± 2.39 |
| **OCT Metrics** | | | |
| RNFL (total) * | 103.5 ± 13.3 | 92.9 ± 12.3 | 70.3 ± 13.7 |
| MRW (total) * | 352.9 ± 57.5 | 282.2 ± 63.8 | 206.3 ± 71.6 |

**Table 2:**
**Intrasession repeatability assessment of ocular blood flow metrics.**

Table reports observed mean ± standard deviation of coefficient of variation (CV, expressed as a percent value) in measurement of various metrics derived from ocular blood flow data at the optic disc, disc vessels, disc perfusion, and fovea regions of interest (ROIs) across multiple cardiac cycles within the same imaging session for healthy (n = 20), glaucoma suspect (n = 16), and glaucoma (n = 10) subjects. Every column of three asterisks (*) indicates that CV of at least one subject group is statistically different ($p < 0.05$, ANOVA). VRI: volumetric rise index, VFI: volumetric fall index, TtR: time-to-rise, TtF: time-to-fall, ATI: acceleration time index, BOT: blow-out time

| Intrasession CV (%) | | Ocular Blood Flow Metrics | | | | | | | | | |
|---|---|---|---|---|---|---|---|---|---|---|---|
| **ROI** | **Subjects** | **Dip** | **Mean** | **Peak** | **VRI** | **VFI** | **TtR** | **TtF** | **Skew** | **ATI** | **BOT** |
| **Optic Disc** | **Healthy Controls** | 2.3 ± 0.9* | 1.8 ± 0.7* | 2.0 ± 0.9 | 8.0 ± 2.9 | 4.5 ± 1.7* | 6.6 ± 2.5 | 3.7 ± 1.3* | 10.2 ± 5.8 | 6.0 ± 2.2 | 3.8 ± 2.1* |
| | **Glaucoma Suspect** | 3.3 ± 1.5* | 2.2 ± 0.9* | 2.2 ± 0.9 | 7.6 ± 2.4 | 4.3 ± 1.4* | 6.6 ± 2.4 | 4.2 ± 1.3* | 10.6 ± 3.2 | 6.0 ± 2.0 | 4.8 ± 1.6* |
| | **Glaucoma** | 4.6 ± 2.7* | 2.7 ± 0.9* | 2.6 ± 1.2 | 8.6 ± 2.7 | 7.4 ± 4.9* | 7.6 ± 2.6 | 7.0 ± 6.3* | 15.5 ± 9.0 | 9.0 ± 5.7 | 6.4 ± 3.3* |
| **Disc Vessel** | **Healthy Controls** | 2.2 ± 0.8* | 1.6 ± 0.7* | 1.8 ± 0.8 | 7.9 ± 2.8 | 4.4 ± 1.6* | 6.6 ± 2.5 | 3.7 ± 1.3* | 13.3 ± 10 | 6.0 ± 2.2 | 4.6 ± 3.0 |
| | **Glaucoma Suspect** | 3.5 ± 1.7* | 2.2 ± 1.0* | 2.0 ± 1.1 | 7.5 ± 2.4 | 4.3 ± 1.5* | 6.6 ± 2.4 | 4.2 ± 1.3* | 15.7 ± 8.3 | 6.0 ± 2.0 | 6.4 ± 3.0 |
| | **Glaucoma** | 4.6 ± 2.8* | 2.6 ± 1.0* | 2.5 ± 1.1 | 8.7 ± 2.7 | 7.4 ± 5.1* | 7.6 ± 2.6 | 7.0 ± 6.3* | 17.9 ± 11.7 | 9.0 ± 5.7 | 7.6 ± 3.7 |
| **Disc Perfusion** | **Healthy Controls** | 2.9 ± 1.0* | 2.2 ± 0.8* | 2.5 ± 1.0 | 8.3 ± 3.0 | 4.7 ± 1.7* | 6.6 ± 2.5 | 3.7 ± 1.3* | 10.1 ± 5.7 | 6.0 ± 2.2 | 3.8 ± 2.1* |
| | **Glaucoma Suspect** | 4.2 ± 1.6* | 2.7 ± 0.8* | 2.8 ± 0.9 | 7.9 ± 2.9 | 4.6 ± 1.3* | 6.6 ± 2.4 | 4.2 ± 1.3* | 10.8 ± 4.7 | 6.0 ± 2.0 | 5.2 ± 1.8* |
| | **Glaucoma** | 5.3 ± 2.8* | 3.0 ± 0.9* | 2.9 ± 1.3 | 8.9 ± 3.0 | 7.3 ± 4.7* | 7.6 ± 2.6 | 7.0 ± 6.3* | 13.8 ± 7.5 | 9.0 ± 5.7 | 6.5 ± 3.1* |
| **Fovea** | **Healthy Controls** | 2.2 ± 0.8 | 1.6 ± 0.6 | 1.7 ± 0.7* | 8.4 ± 3.3 | 5.0 ± 2.4 | 7.3 ± 3.2 | 4.3 ± 2.2 | 13.3 ± 7.0 | 7.3 ± 3.4 | 4.1 ± 1.5* |
| | **Glaucoma Suspect** | 2.5 ± 1.4 | 1.9 ± 0.7 | 2.3 ± 0.8* | 8.4 ± 2.1 | 5.5 ± 2.5 | 7.2 ± 2.0 | 5.1 ± 3.1 | 20.4 ± 11.5 | 7.0 ± 2.0 | 7.9 ± 3.4* |
| | **Glaucoma** | 3.4 ± 2.6 | 2.3 ± 1.0 | 2.9 ± 1.3* | 9.0 ± 4.2 | 6.7 ± 6.9 | 6.4 ± 3.5 | 5.9 ± 7.7 | 13.1 ± 7.4 | 7.7 ± 3.8 | 7.4 ± 2.5* |

**Table 3:**
**Intersession repeatability assessment of ocular blood flow metrics.**

Table reports observed mean ± standard deviation of coefficient of variation (CV, expressed as a percent value) in measurement of various metrics derived from BFVi data at the optic disc, disc vessels, disc perfusion, and fovea regions of interest (ROI) across multiple imaging sessions for healthy (n = 20), glaucoma suspect (n = 16), and glaucoma (n = 10) subjects. Every column of three asterisks (*) indicate that CV of at least one subject group is statistically different ($p < 0.05$, ANOVA).
VRI: volumetric rise index, VFI: volumetric fall index, TtR: time-to-rise, TtF: time-to-fall, ATI: acceleration time index, BOT: blow-out time

| Intersession CV (%) | | Ocular Blood Flow Metrics | | | | | | | | | |
|---|---|---|---|---|---|---|---|---|---|---|---|
| **ROIs** | **Subjects** | **Dip** | **Mean** | **Peak** | **VRI** | **VFI** | **TtR** | **TtF** | **Skew** | **ATI** | **BOT** |
| **Optic Disc** | **Healthy Controls** | 6.5 ± 3.4 | 5.8 ± 3.1 | 5.4 ± 3.2 | 7.6 ± 3.6 | 7.8 ± 5.1 | 4.1 ± 2.6 | 4.6 ± 3.3 | 8.6 ± 6.1 | 4.6 ± 2.5 | 2.8 ± 1.7 |
| | **Glaucoma Suspect** | 7.4 ± 3.7 | 6.5 ± 3.3 | 6.0 ± 3.2 | 7.7 ± 3.4 | 7.4 ± 3.4 | 4.4 ± 2.9 | 4.9 ± 1.2 | 7.1 ± 5.6 | 5.1 ± 2.6 | 4.2 ± 2.9 |
| | **Glaucoma** | 7.0 ± 3.8 | 5.9 ± 2.9 | 5.7 ± 2.5 | 10.7 ± 3.8 | 7.7 ± 4.1 | 6.7 ± 4.4 | 5.2 ± 4.7 | 11.2 ± 4.6 | 5.5 ± 3.9 | 4.6 ± 2.1 |
| **Disc vessel** | **Healthy Controls** | 6.4 ± 3.1 | 5.7 ± 3.0 | 5.3 ± 3.2 | 7.3 ± 3.4* | 7.6 ± 5.5 | 4.1 ± 2.6 | 4.6 ± 3.3 | 9.9 ± 5.2 | 4.6 ± 2.5 | 3.1 ± 1.9 |
| | **Glaucoma Suspect** | 7.3 ± 3.7 | 6.3 ± 3.3 | 5.7 ± 3.0 | 7.6 ± 3.7* | 7.1 ± 3.3 | 4.4 ± 2.9 | 4.9 ± 1.2 | 14.6 ± 14.7 | 5.1 ± 2.6 | 5.4 ± 3.6 |
| | **Glaucoma** | 7.5 ± 3.9 | 6.6 ± 2.8 | 6.4 ± 2.2 | 10.9 ± 3.2* | 8.5 ± 4.2 | 6.7 ± 4.4 | 5.2 ± 4.7 | 12.0 ± 8.1 | 5.5 ± 3.9 | 5.6 ± 2.9 |
| **Disc Perfusion** | **Healthy Controls** | 7.1 ± 3.4 | 6.5 ± 3.1 | 6.2 ± 3.2 | 8.4 ± 3.5 | 8.3 ± 4.7 | 4.1 ± 2.6 | 4.6 ± 3.3 | 8.0 ± 6.0 | 4.6 ± 2.5 | 3.3 ± 2.6 |
| | **Glaucoma Suspect** | 7.8 ± 5.0 | 7.1 ± 4.4 | 6.9 ± 4.2 | 8.2 ± 3.7 | 8.1 ± 3.9 | 4.4 ± 2.9 | 4.9 ± 1.2 | 7.4 ± 3.9 | 5.1 ± 2.6 | 4.0 ± 2.6 |
| | **Glaucoma** | 7.1 ± 4.0 | 6.2 ± 3.5 | 6.1 ± 3.3 | 11.0 ± 3.8 | 7.5 ± 4.3 | 6.7 ± 4.4 | 5.2 ± 4.7 | 11.1 ± 4.9 | 5.5 ± 3.9 | 5.1 ± 3.1 |
| **Fovea** | **Healthy Controls** | 6.0 ± 3.0 | 5.5 ± 3.0 | 5.3 ± 3.1 | 8.2 ± 5.7 | 6.9 ± 3.3 | 5.3 ± 4.7 | 5.4 ± 3.0 | 7.8 ± 4.8* | 6.1 ± 4.9* | 3.2 ± 2.8* |
| | **Glaucoma Suspect** | 6.2 ± 2.9 | 5.6 ± 2.9 | 5.5 ± 3.0 | 7.8 ± 3.9 | 5.7 ± 3.6 | 4.8 ± 2.6 | 3.9 ± 2.0 | 13.0 ± 8.3* | 3.9 ± 2.0* | 5.4 ± 2.9* |
| | **Glaucoma** | 6.9 ± 5.0 | 5.9 ± 3.9 | 5.6 ± 3.5 | 6.9 ± 5.1 | 6.1 ± 3.5 | 3.3 ± 2.4 | 3.2 ± 2.5 | 5.5 ± 3.5* | 2.8 ± 1.5* | 2.8 ± 1.6* |

**Table 4:**

**Comparison of ocular blood flow metrics in healthy, glaucoma suspect, and glaucomatous eyes.**

Table reports observed blood flow velocity index (BFVi) metrics (mean ± standard deviation) in specific ocular regions (optic disc, disc vessels, disc perfusion, fovea) of healthy (n = 20), glaucoma suspect (n = 16), and glaucoma (n = 10) subjects. Rows with an asterisk (*) indicate statistical differences in the metrics obtained from the three subject groups ($p < 0.05$, ANOVA).
VRI: volumetric rise index, VFI: volumetric fall index, TtR: time-to-rise, TtF: time-to-fall, ATI: acceleration time index, BOT: blow-out time

| Assessed Regions | BFVi Metrics | Units | Healthy Controls | Glaucoma Suspects | Glaucoma |
|---|---|---|---|---|---|
| | | | n = 20 subjects | n = 16 subjects | n = 10 subjects |
| Optic Disc | Dip* | a.u. | 7.3 ± 1.9 | 6.0 ± 0.9 | 5.0 ± 1.8 |
| | Mean* | a.u. | 8.9 ± 2.3 | 7.5 ± 1.2 | 6.4 ± 2.0 |
| | Peak* | a.u. | 10.4 ± 2.6 | 8.9 ± 1.5 | 7.8 ± 2.4 |
| | VRI* | a.u. | 2.3 ± 0.6 | 2.0 ± 0.4 | 1.7 ± 0.5 |
| | VFI* | a.u. | 5.1 ± 1.6 | 4.0 ± 0.9 | 3.5 ± 1.4 |
| | TtR | ms | 267.5 ± 30.6 | 269.1 ± 23.9 | 280.2 ± 36.3 |
| | TtF | ms | 583.0 ± 125.0 | 542.8 ± 82.0 | 557.0 ± 142.8 |
| | Skew | - | 0.7 ± 0.1 | 0.7 ± 0.1 | 0.7 ± 0.1 |
| | ATI | - | 0.3 ± 0.0 | 0.3 ± 0.0 | 0.3 ± 0.0 |
| | BOT | - | 0.5 ± 0.0 | 0.5 ± 0.0 | 0.5 ± 0.0 |
| Disc Vessels | Dip* | a.u. | 9.9 ± 1.7 | 9.2 ± 1.2 | 7.6 ± 2.0 |
| | Mean* | a.u. | 11.7 ± 1.9 | 11.0 ± 1.4 | 9.3 ± 1.9 |
| | Peak* | a.u. | 13.5 ± 2.2 | 12.8 ± 1.8 | 11.1 ± 2.1 |
| | VRI | a.u. | 3.1 ± 0.5 | 2.9 ± 0.4 | 2.6 ± 0.6 |
| | VFI* | a.u. | 6.8 ± 1.5 | 6.0 ± 1.2 | 5.1 ± 1.6 |
| | TtR | ms | 267.5 ± 30.6 | 269.1 ± 23.9 | 280.2 ± 36.3 |
| | TtF | ms | 583.0 ± 125.0 | 542.8 ± 82.0 | 557.0 ± 142.8 |
| | Skew | - | 0.6 ± 0.1 | 0.7 ± 0.1 | 0.7 ± 0.1 |
| | ATI | - | 0.3 ± 0.0 | 0.3 ± 0.0 | 0.3 ± 0.0 |
| | BOT | - | 0.5 ± 0.0 | 0.5 ± 0.0 | 0.5 ± 0.0 |
| Disc Perfusion | Dip* | a.u. | 4.9 ± 2.0 | 3.7 ± 0.7 | 3.4 ± 1.3 |
| | Mean* | a.u. | 6.3 ± 2.4 | 4.9 ± 1.0 | 4.6 ± 1.6 |
| | Peak | a.u. | 7.6 ± 2.8 | 6.0 ± 1.4 | 5.8 ± 2.0 |
| | VRI | a.u. | 1.6 ± 0.6 | 1.3 ± 0.3 | 1.2 ± 0.4 |
| | VFI* | a.u. | 3.6 ± 1.6 | 2.6 ± 0.7 | 2.5 ± 1.1 |
| | TtR | ms | 267.5 ± 30.6 | 269.1 ± 23.9 | 280.2 ± 36.3 |
| | TtF | ms | 583.0 ± 125.0 | 542.8 ± 82.0 | 557.0 ± 142.8 |
| | Skew | - | 0.7 ± 0.2 | 0.8 ± 0.2 | 0.8 ± 0.1 |
| | ATI | - | 0.3 ± 0.0 | 0.3 ± 0.0 | 0.3 ± 0.0 |

| Assessed Regions | BFVi Metrics | Units | Healthy Controls | Glaucoma Suspects | Glaucoma |
|---|---|---|---|---|---|
| | | | n = 20 subjects | n = 16 subjects | n = 10 subjects |
| | **BOT** | - | 0.5 ± 0.0 | 0.4 ± 0.0 | 0.4 ± 0.0 |
| **Fovea** | **Dip** | a.u. | 6.4 ± 3.8 | 4.4 ± 2.1 | 3.8 ± 1.7 |
| | **Mean** | a.u. | 7.6 ± 4.2 | 5.5 ± 2.7 | 5.2 ± 2.1 |
| | **Peak** | a.u. | 8.7 ± 4.7 | 6.7 ± 3.3 | 6.6 ± 2.7 |
| | **VRI** | a.u. | 1.9 ± 1.0 | 1.4 ± 0.7 | 1.4 ± 0.7 |
| | **VFI** | a.u. | 4.4 ± 2.3 | 3.1 ± 1.6 | 3.0 ± 1.7 |
| | **TtR** | ms | 264.6 ± 28.2 | 267.7 ± 25.5 | 267.8 ± 30.1 |
| | **TtF** | ms | 606.6 ± 125.1 | 559.1 ± 83.0 | 582.7 ± 143.2 |
| | **Skew*** | - | 0.7 ± 0.2 | 0.8 ± 0.2 | 0.9 ± 0.1 |
| | **ATI** | - | 0.3 ± 0.0 | 0.3 ± 0.0 | 0.3 ± 0.0 |
| | **BOT*** | - | 0.7 ± 0.1 | 0.8 ± 0.0 | 0.9 ± 0.0 |

**Table 5.**

**Results of multi-variable regression analysis.**

Beta coefficients for the effect of glaucoma subject relative to control on parameter estimate in multiple variable regression model accounting for sex and age. (* indicates coefficient p value < 0.05 by Wald test, bold font indicates that p < 0.05 for the effect of glaucoma suspect versus glaucoma, ǂ indicates coefficient when dependent variable was log-transformed)

| **Differences in Mean Parameter Values in Glaucoma vs Control Subjects** | | | |
|---|---|---|---|
| **Parameters** | **Optic Disc** | **Disc Vessels** | **Disc Perfusion** |
| Peak | −2.85* | **−2.54*** | −2.14* |
| Dip | −2.0* | **−1.9*** | −0.33*,ǂ |
| Mean | −2.43* | **−2.22*** | −1.76* |
| Volumetric Rise Index | −0.68* | **−0.62*** | −0.33*,ǂ |
| Volumetric Fall Index | −1.56* | **−1.49*** | −0.37*,ǂ |
| Time-to-Rise | 0.07 | 0.07 | 0.07 |
| Time-to-Fall | −22.82 | −22.82 | −22.82 |
| Skew | −0.08* | −0.08* | −0.08 |
| Acceleration Time Index | 0.009 | 0.009 | 0.009 |
| Blow-out time | 0.03* | 0.006 | 0.02 |